Astron. Astrophys. 351, L1–L4 (1999)

ASTRONOMY AND ASTROPHYSICS

LETTER

Letter to the Editor

The young detached CO shell around U Camelopardalis

M. Lindqvist[1], **H. Olofsson**[2], **R. Lucas**[3], **F.L. Schöier**[2], **R. Neri**[3], **V. Bujarrabal**[4], **and C. Kahane**[5]

[1] Onsala Space Observatory, 43992 Onsala, Sweden
[2] Stockholm Observatory, 13336 Saltsjöbaden, Sweden
[3] IRAM, 300 rue de la Piscine, 38406 St Martin d'Heres Cedex, France
[4] Observatorio Astronómico Nacional, Apartado 1143, 28800 Alcalá de Henares, Spain
[5] Observatoire de Grenoble, B.P. 53, 38041 Grenoble Cedex 9, France

Received 8 September 1999 / Accepted 11 October 1999

Abstract. We report IRAM Plateau de Bure interferometer observations of the carbon star U Cam in the $\mathrm{CO}(J=1\rightarrow0)$ and $\mathrm{CO}(J=2\rightarrow1)$ lines. The remarkable images show that U Cam is surrounded by a geometrically thin, $\sim10^{16}$ cm, shell of gas at a distance of $\sim6\times10^{16}$ cm from the star, that expands with a velocity of $\sim23\,\mathrm{km\,s^{-1}}$. The estimated mass of the shell is low, $\sim10^{-3}\,\mathrm{M_\odot}$. In addition, we detect emission that peaks at the stellar position. From this we estimate a present mass loss rate and gas expansion velocity of $\sim2.5\times10^{-7}\,\mathrm{M_\odot\,yr^{-1}}$ and $12\,\mathrm{km\,s^{-1}}$, respectively. One possible explanation to the structure of the circumstellar medium is that the shell was produced during a very short period, ~150 yr, of high mass loss rate, $\sim10^{-5}\,\mathrm{M_\odot\,yr^{-1}}$, about 800 yr ago. U Cam may fit into the scenario where a helium-shell flash modulates the mass loss rate on short times scales.

Key words: stars: carbon – stars: circumstellar matter – stars: individual: U Cam – stars: mass-loss

1. Introduction

U Cam is a semi-regularly variable carbon star with "normal" optical properties (Lambert et al. 1986). Radio observations, however, indicate that its circumstellar envelope has a remarkable morphology, suggesting a variation of the mass loss rate on a time scale as short as $\sim10^3$ yr (Bujarrabal & Cernicharo 1994; Lindqvist et al. 1996; Neri et al. 1998). This may be related to the geometrically thin CO shells seen around four optically bright carbon stars (Olofsson et al. 1996, 1998). Previous studies of U Cam, however, lacked the angular resolution needed to put constraint on the mass loss rate and its variation with time.

In this *Letter* we address this problem by presenting a preliminary analysis of CO radio line brightness distributions towards U Cam obtained with the IRAM Plateau de Bure (PdB) interferometer. The distance to U Cam is assumed to be 500 pc (Olofsson et al. 1993a).

Send offprint requests to: M. Lindqvist

2. Observations and data reduction

The $\mathrm{CO}(J=1\rightarrow0;\ 115.271\,\mathrm{GHz})$ and $\mathrm{CO}(J=2\rightarrow1;\ 230.538\,\mathrm{GHz})$ observations of U Cam were made simultaneously between April 1998 and March 1999 using the IRAM PdB interferometer, France (including also the $\mathrm{HC_3N}(J=25\rightarrow24)$ line at 227.419 GHz). The data were obtained using five configurations (A, B2, B1, C1, and D). The phase-calibrators were B0224+671 and NRAO150. 0923+392 was used for bandpass calibration, and MWC349 as flux calibrator. The GILDAS package, the XS package (P. Bergman, Onsala Space Observatory), and the NRAO AIPS package, were used to calibrate and analyse the data. The images were made, using natural weighting, with a channel separation of $\sim1.0\,\mathrm{km\,s^{-1}}$.

3. Results

The $\mathrm{CO}(J=1\rightarrow0)$ and $\mathrm{CO}(J=2\rightarrow1)$ data are presented in Figs 1 and 2. The velocity-channel maps, averaged to a channel separation of $\sim5.0\,\mathrm{km\,s^{-1}}$, reveal remarkable brightness distributions. First, they show clearly that U Cam is surrounded by a geometrically thin shell of CO line-emitting gas. Second, they show emission that peaks at the stellar position, most likely this originates from the present mass loss gas. Hence, a CO envelope morphology very similar to that found by Olofsson et al. (1996, 1998) towards a few other carbon stars. It contrasts strongly with the CO brightness distributions normally seen towards AGB stars (Neri et al. 1998).

The possibility of missing flux in our interferometric data has been investigated by comparing the integrated (over the map) interferometer spectra with single-dish data [observed with the IRAM 30 m telescope, Neri et al. (1998)], see Figs 2c and 2d. We conclude that we are able to recover about 52% and 48% (corrections to the interferometer data for the primary beam response results in 54% and 57%, respectively) of the total flux of the $J=1\rightarrow0$ and $J=2\rightarrow1$ lines, respectively. Merging with existing single-dish data (Neri et al. 1998) is not worthwhile due to their lower quality.

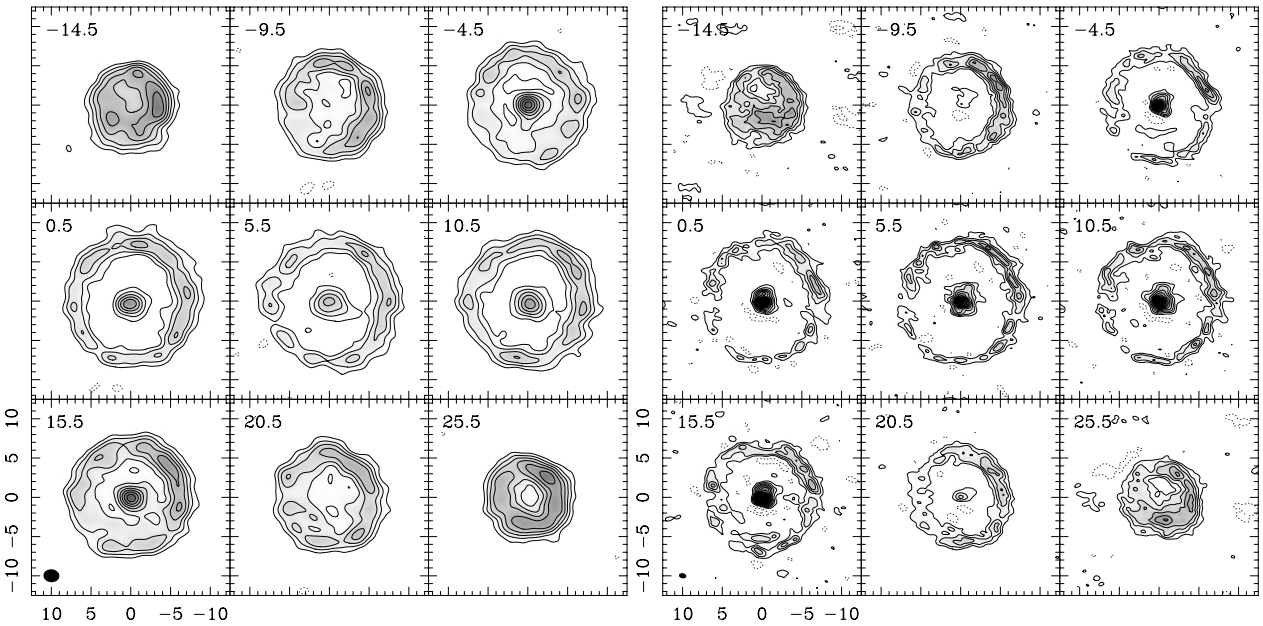

Fig. 1. Velocity-channel maps (Δv∼5.0 km s^{-1}) of the CO($J = 1 \rightarrow 0$) (left panels) and CO($J = 2 \rightarrow 1$) (right panels) emission towards U Cam. The central LSR velocity of each channel is given in the upper left corner. The coordinates are relative to $\alpha(J2000) = 03^{\rm h}41^{\rm m}48\overset{\rm s}{.}167$ and $\delta(J2000) = 62^\circ38'54\overset{''}{.}49$. Units are arcseconds. Contours range from -0.045 to 0.18 by 0.015 Jy beam^{-1} and -0.10 to 0.50 by 0.025 Jy beam^{-1} for the $J = 1 \rightarrow 0$ and $J = 2 \rightarrow 1$ data, respectively (zero is omitted). Negative contours are dashed. A brightness temperature of 1 K corresponds to 37 mJy beam^{-1} and 27 mJy beam^{-1} for $J = 1 \rightarrow 0$ and $J = 2 \rightarrow 1$, respectively. The synthesized CLEAN beam [shown at the half power contour (filled) in the lower left corner] is $2\overset{''}{.}01 \times 1\overset{''}{.}65$ (PA=+85°) and $0\overset{''}{.}95 \times 0\overset{''}{.}65$ (PA=+77°) for the $J = 1 \rightarrow 0$ and $J = 2 \rightarrow 1$ data, respectively

3.1. The shell emission

The shell emission appears to have an overall spherical symmetry, although deviations are traceable, Fig. 1. In particular, the brightness distributions are asymmetric with considerably stronger emission in the NW than in the SE. However, this asymmetry appears to have no effect on the overall circular symmetry of the shell emission, i.e., the gas expansion velocity appears to be the same in all directions. The brightness distributions are very patchy, suggesting a high degree of clumpiness of the medium. We find no displacement between the position of the centroid of the shell emission and the position of the star. The centroid lies within $\sim$0$\overset{''}{.}$1 of the stellar Hipparcos position (see below). Using the spectra at the centre pixel (Figs 2a and 2b; note that the inner U-shaped feature originates in the present mass loss gas) we estimate that the outer blue- and redshifted emission peaks occur at about -16.5 and 29.5 km s^{-1}, respectively. From this we derive a gas expansion velocity, $v_{\rm e}$, of 23.0 km s^{-1} and a systemic velocity, v_*, of 6.5 km s^{-1}. The systemic velocity agrees with that estimated from the central emission (see below).

We have computed azimuthal averages of the data close to the systemic velocity ($v_* \pm 1.0$ km s^{-1}) using concentric annuli around the centre position. The width of each annulus is the pixel size in the map. The resulting radial brightness profiles are presented in Figs 2g and 2h. Both shell emissions peak at about the same distance from the star. The width and the radius of the shell have been determined in the image domain by fitting a ring, with a Gaussian distribution in the radial direction, to individual channel maps. We excluded the emission from the feature peaking at the centre while fitting. We derive, at the systemic velocity ($v_* \pm 1.0$ km s^{-1}), a radius, $R_{\rm s}$, of $\sim$7$\overset{''}{.}$3 and $\sim$7$\overset{''}{.}$4 from the $J = 1 \rightarrow 0$ and $J = 2 \rightarrow 1$ data, respectively. The shell widths (FWHM:s), $\Delta R_{\rm s}$, are $\sim$2$\overset{''}{.}$5 and $\sim$1$\overset{''}{.}$4 from the $J = 1 \rightarrow 0$ and $J = 2 \rightarrow 1$ data, respectively. Using circular beam sizes of 1$\overset{''}{.}$82 ($J = 1 \rightarrow 0$) and 0$\overset{''}{.}$79 ($J = 2 \rightarrow 1$) the resulting deconvolved widths are 1$\overset{''}{.}$7 and 1$\overset{''}{.}$2. Thus, the shell appears broader in the $J = 1 \rightarrow 0$ line but one should be cautious when measuring sizes smaller than the beam, i.e., using overresolution in interferometry. The sizes of the shell, as a function of line-of-sight velocity, $v_{\rm z}$, are presented in Figs 2e and 2f. We have overlaid the simple relation, $R(v_{\rm z}) = R_{\rm s}[1-((v_{\rm z}-v_*)/v_{\rm e})^2]^{1/2}$ (this relation should apply if the shell is spherical and expands with a constant velocity). Good fits are obtained for $R_{\rm s} = 7\overset{''}{.}3$, $v_* = 6.0$ km s^{-1}, and $v_{\rm e} = 23.0$ km s^{-1}, i.e. results in very good agreement with those obtained from the spectra. However, the data deviate significantly in certain velocity intervals, most notably around -4.5 and $+15.5$ km s^{-1} (this is close to the extreme velocities of the centre emission, but we do not believe that this has an effect). One possible reason is the presence of weak emission inside the shell, see e.g. the CO($J = 2 \rightarrow 1$) velocity-channel maps at -4.5 and $+15.5$ km s^{-1}. It is unlikely that the emission inside the shell is a result of the deconvolution procedure since we obtain similar results if we model the data directly in the Fourier plane. We find also that similar deviations can be seen in the HCN($J = 1 \rightarrow 0$) maps presented by Lindqvist

et al. (1996). This may indicate an even more complex envelope structure.

In summary, we find a shell radius and width of $\sim 7\farcs3$ (5.5×10^{16} cm) and $\sim 1\farcs5$ (1.1×10^{16} cm), respectively. Hence, we may conclude that the CO emitting shell was produced $R_{\rm s}/v_{\rm e} \sim 800\,{\rm yr}$ ago (provided that the expansion velocity can be used to estimate the time scale) during a period of $\Delta R_{\rm s}/v_{\rm e} \sim 150\,{\rm yr}$ (provided that e.g. no effects of interacting winds are present). The shell sizes estimated from the HCN($J=1\rightarrow0$) and CN($N=1\rightarrow0$) data by Lindqvist et al. (1996), who applied model fits to the data in the Fourier plane, are consistent with that determined here.

3.2. The central emission

We have determined the position of the centre emission, i.e., the compact feature peaking at the centre (Fig. 1), by fitting a Gaussian model to the $J=2\rightarrow1$ channel maps. The result, at the systemic velocity, is $\alpha(J2000) = 03^{\rm h}41^{\rm m}48\fs13$ and $\delta(J2000) = 62\degr38\arcmin54\farcs5$. The errors obtained from the model fit are $\sim0\farcs1$ in both α and δ. The position agrees, within the absolute positional uncertainty of $\leq0\farcs5$, with the Hipparcos position of U Cam, $\alpha(J2000) = 03^{\rm h}41^{\rm m}48\fs17$ and $\delta(J2000) = 62\degr38\arcmin54\farcs4$.

The spectra of the centre emission at the centre pixel show U-shaped features (Figs 2a and 2b; the outer peaks are due to the shell emission), which indicate resolved, optically thin emission. The expansion velocity estimated from these spectra is considerably lower than that of the outer shell, $v_{\rm e}\sim12\,{\rm km\,s^{-1}}$, for both the $J=1\rightarrow0$ and $J=2\rightarrow1$ data. This is consistent with the results from other emissions, e.g., SiO($J=3\rightarrow2$) and CS($J=5\rightarrow4$) (Bujarrabal & Cernicharo 1994). In addition, our PdB observations of the HC_3N($J=25\rightarrow24$) line, shows emission from the inner envelope only. The estimated systemic velocity of the central emission is $6.5\,{\rm km\,s^{-1}}$, i.e., the shell and the centre emission have, within the errors, the same systemic velocity.

To estimate the sizes of the emitting regions we fitted Gaussian functions to the radial brightness profiles (within $4''$ of the centre) presented in Figs 2g and 2h (this may in fact be a too simplistic approach since the $J=2\rightarrow1$ emission shows signs of asymmetry in the NS direction). The results at $v_*\pm1.0\,{\rm km\,s^{-1}}$ are FWHM:s of $\sim3\farcs3$ and $\sim2\farcs4$ for the $J=1\rightarrow0$ and $J=2\rightarrow1$ data, respectively. This corresponds to deconvolved sizes of $\sim2\farcs8$ and $\sim2\farcs3$.

3.3. Radiative transfer analysis

We have made a preliminary analysis of the data using a non-LTE radiative transfer code based on the Monte-Carlo method (Schöier 1999, PhD thesis, in prep.). The central emission data are consistent with a present mass loss rate of $2.5\times10^{-7}\ {\rm M_\odot\,yr^{-1}}$ and a gas expansion velocity of $12\,{\rm km\,s^{-1}}$. The size estimates and line intensities were used as constraints, and a CO abundance with respect to H_2, $f_{\rm CO}$, of 10^{-3} was adopted (the energy balance of the gas is included). The best fit

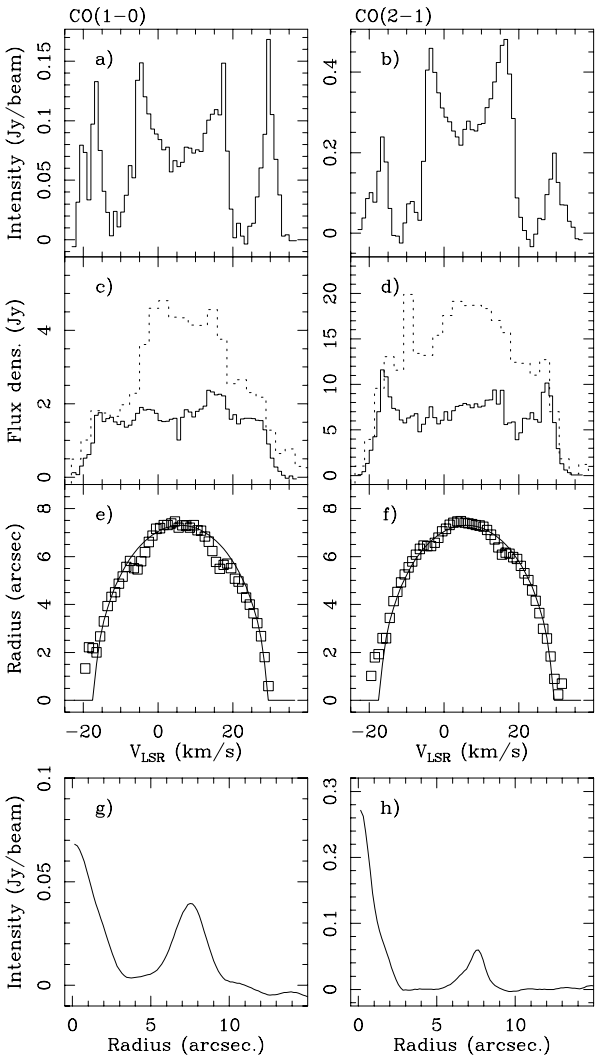

Fig. 2. a Interferometer $CO(J=1\rightarrow0)$ and **b** $CO(J=2\rightarrow1)$ spectra at the map centre. Comparison of integrated (over the maps) interferometer **c** $CO(J=1\rightarrow0)$ and **d** $CO(J=2\rightarrow1)$ spectra (*solid lines*) and integrated spectra calculated from maps obtained with the IRAM 30 m telescope (*dashed lines*; Neri et al. 1998). Size estimates of the shell for the **e)** $CO(J=1\rightarrow0)$ and **f)** $CO(J=2\rightarrow1)$ data. The lines give the relation $R(v_{\rm z}) = R_{\rm s}[1-((v_{\rm z}-v_*)/v_{\rm e})^2]^{1/2}$ with $v_{\rm e} = 23.0\,{\rm km\,s^{-1}}$, $v_* = 6.0\,{\rm km\,s^{-1}}$, and $R_{\rm s} = 7\farcs3$. Radial brightness profiles of the **g** $CO(J=1\rightarrow0)$ and **h** $CO(J=2\rightarrow1)$ emission close to the systemic velocity $(v_*\pm1.0\,{\rm km\,s^{-1}})$

was obtained for a CO envelope radius smaller (by ∼50%) than predicted by the CO photodissociation model of Mamon et al. (1988). Nevertheless, considering the uncertanties in the excitation and photodissociation models, we conclude that the central CO brightness distributions are consistent with their outer radii being determined by photodissociation.

For the outer gas we have estimated the H_2 density, $n_{\rm H_2}$, and the kinetic temperature, $T_{\rm k}$, assuming uniform density and temperature in the shell. In addition to the interferometer data (the spectra at the map centre), we used single dish $J=1\rightarrow0$, $J=2\rightarrow1$, and $J=3\rightarrow2$ (obtained from the JCMT archive)

spectra to find the best fit model. A reasonable fit to the data can be found for a range of values (mainly due to the lack of constrains, but also the calibration uncertainties in the single dish data and the missing flux in the interferometer data play a role), but $n_{\rm H_2}\sim 2\times10^3\,{\rm cm}^{-3}$ (which may be a lower limit since HCN is detected in the shell; Lindqvist et al. 1996) and $T_{\rm k}\sim$60 K is adopted in this paper (we used the same $f_{\rm CO}$ as Olofsson et al. (1998) did for TT Cyg, 10^{-3}, see below). The uncertainties are probably a factor of 2 and 3 for $n_{\rm H_2}$ and $T_{\rm k}$, respectively. This leads to a shell mass, $M_{\rm shell}$, of $1\times10^{-3}\,{\rm M}_\odot$, and a mass loss rate of $M_{\rm shell}v_{\rm e}/\Delta R_{\rm s}\sim 9\times10^{-6}\ {\rm M}_\odot\,{\rm yr}^{-1}$ (assuming that all the shell material was ejected during a period that can be estimated using the gas expansion velocity). The outer radius of the shell emission is much smaller than the CO photodissociation radius corresponding to the estimated mass loss rate, $\sim4\times10^{17}$ cm, suggesting that also the density drops sharply at this radius. Thus, we belive that the CO brightness distributions trace the density distribution relatively well.

4. Discussion and conclusions

The circumstellar gas around U Cam seems to have much in common with the geometrically thin, CO line-emitting shells of gas around four other carbon stars, R Scl, U Ant, S Sct, and TT Cyg (Olofsson et al. 1996). These shells have been interpreted as due to a considerable modulation of the mass loss rate on short time scales. A process that possibly affect the mass loss properties of the star is the helium-shell flash (a thermal pulse). Even moderate changes in radius, effective temperature, and luminosity may lead to considerable changes in the mass loss rate over a time scale of 10^{3-4} yr, possibly periodic on a time scale of 10^{4-5} yr (e.g., Olofsson et al. 1990; Blöcker 1995; Schröder et al. 1998). There are potential problems with this interpretation. In particular, an interacting wind scenario, in which a faster wind runs into a slower wind and the matter piles up, is not unlikely since the star very likely had a mass loss also prior to the ejection. In this case the estimated mass loss rate loses significance, and so does the time scales.

A way to investigate this problem is to observe CO shells of very different ages. In this respect the clear detection of a young CO shell around U Cam is very important. This shell has an age of only $\sim$800 yr whereas the age of e.g. the TT Cyg shell (the only object observed with comparable spatial resolution) is close to 10^4 yr. Nevertheless, the linear widths of these shells are roughly the same, $\sim10^{16}$ cm. There are, though, some notable differences. Most important is the shell mass. The result for U Cam, $\sim10^{-3}\,{\rm M}_\odot$, is considerably lower than Olofsson (1998) found for TT Cyg, $0.024\,{\rm M}_\odot$ (or $0.007\,{\rm M}_\odot$ for a smaller distance; similar shell masses have been estimated for the three other stars). The difference could be due to a weaker thermal pulse in the case of U Cam, or the effects of swept-up matter in the other four cases. In U Cam the present mass loss rate, $2.5\times10^{-7}\ {\rm M}_\odot\,{\rm yr}^{-1}$, and gas expansion velocity, $12\,{\rm km\,s}^{-1}$, are relatively high compared to a $\rm few\times10^{-8}\ M_\odot\,yr^{-1}$ and $\sim5\,{\rm km\,s}^{-1}$ for TT Cyg and the other stars. The high expansion velocity and the mass loss rate of the present mass loss gas can be due to the thermal pulse in U Cam being relatively recent. Naturally, the derived quantities depend on the distance uncertainty [compared to Hipparcos distances, the method used by Olofsson et al. (1993a) tend to give larger distances]. A smaller distance would lower the present mass loss and the shell mass. Note that, irrespective of the distance U Cam will have a different relation between the present mass loss rate and the shell mass than TT Cyg.

The U Cam shell has the advantage of being detectable in other circumstellar molecular species than CO (Olofsson et al. 1993b; Bujarrabal & Cernicharo 1994; Lindqvist et al. 1996). The only carbon star with a clearly detached CO shell in which Olofsson et al. (1996) also detected other emissions is R Scl. In both cases the shells are young and the excitation is still efficient and the effects of photodissociation less.

Dedication. This paper is dedicated to the victims and their families of the tragic accident of the téléphérique, that gave access to the Plateau de Bure observatory, on July 1st, 1999.

References

Blöcker T. 1995, A&A 297, 727
Bujarrabal V., Cernicharo J., 1994, A&A 288, 551
Lambert D.L., Gustafsson B., Eriksson K., Hinkle K.H., 1986, ApJS 62, 373
Lindqvist M., Lucas R., Olofsson H., et al., 1996, A&A 305, L57
Mamon G.A., Glassgold A.E., Huggins P.J., 1988, ApJ 328, 797
Neri R., Kahane, C., Lucas R., Bujarrabal V., Loup C., 1998, A&AS 130, 1
Olofsson H., Carlström U., Eriksson K., Gustafsson B., Willson L.A., 1990, A&A 230, L13
Olofsson H., Eriksson K., Gustafsson B., Carlström U., 1993a, ApJS 87, 267
Olofsson H., Eriksson K., Gustafsson B., Carlström U., 1993b, ApJS 87, 305
Olofsson H., Bergman P., Eriksson K., Gustafsson B., 1996, A&A 311, 587
Olofsson H., Bergman P., Lucas R., et al., 1998, A&A 330, L1
Schröder K.-P., Winters J.M., Arndt T.U., Sedlmayr E., 1998, A&A 335, L9